International Journal of Mechanical Engineering and Research, ISSN 0973-4562 Vol. 5 No.1 (2015)

FINITE ELEMENTSIMULATION IN ORTHOGONAL MACHINING OF INCONEL 718 ALLOY

P.DEEPAGANESH. ME CAD/CAM, Shanmuganathan Engineering College, Pudukottai.

ABSTRACT

Knowing the stringent operating conditions to which super alloys are subjected to in automobile, aerospace and gas turbine industries, their efficient machining and generation of machined surface with integrity assumes a lot of importance. Considerable attention has been given to the use of ceramic tools for improving productivity in the machining of heat resistant super alloy (HRSA) in recent years. However, because of their negative influence on the surface integrity, ceramic tools are generally avoided particularly for finishing applications. The high end manufactures are more or less dependent on carbide cutting tools for finishing operations. In this present investigation, finite element analysis (FEA) of machining of Inconel 718 Super alloy is carried out using DEFORM 2D. Orthogonal cutting experiments are carried out on a cylindrical bar of Inconel 718 with a cutting speed 50 m/min, feed rate of 0.1 mm/rev and nose radius of 0.6, 0.8 & 1.0 mm. The Johnson-Cook (J-C) constitutive equation is implemented in the finite element code to study the behavior of Inconel 718 during the machining process. The FE results for effective stress, strain, temperature and damage are analyzed. The simulation results showed that the chip segmentation is not occurred at the low cutting speed Damage distribution is large in the case of 0.6 mm tool nose radius compared with other nose radius values. Residual stress measurements are a powerful evaluation criterion for selecting the proper cutting tools because of their sensitiveness of variations in tool parameters.

1. INTRODUCTION

Nickel-based super alloy development of aerospace began in the 1930s. Need for the more creep resistant material than the available austenitic stainless steel propelled research to develop new super alloy. The principal characteristics of nickel as an alloy base are highly phase stability of Face Centered Cubic(FCC) nickel matrix and outstanding strength retention up to 0.7Tm (melting point). These characteristics encourage use of nickel based super alloys in vast number of applications subjected high temperatures. Commercially available nickel base super alloys include inconel, nimonic, rene, udimet, and pyromet. Inconel 718 is the most frequently used nickel based super alloys; hence this study is focused on an investigation into the mechanics of machining inconel 718.

1.1 MACHINING OF NICKEL BASED SUPERALLOYS

Nickel based alloys work-harden rapidly. Work hardening results in strengthening of the

Material. Plastic deformation during machining leads to heat generation. High temperature gradients are localized in narrow bands along shear plane due to poor thermal properties of inconel 718, leading to weakening the material in the deformation zone. Water-base fluids are preferred in high speed turning, milling and grinding because of their greater cooling effect. For slower operations, such as drilling, boring, tapping and broaching heavy lubricants and very rich mixtures of chemical solutions are needed. Tool geometry and machining parameters play important role in evaluating machining efficiency in machining inconel 718. Single point cutting tool with positive rake angles (0^0 for roughing and 8^0 for finishing) are

recommended in turning so that metal is cut instead of ploughed.

2.1 WORKPIECE AND TOOL MATERIAL INCONEL 718

It is difficult to shape as well as machining Inconel 718 using traditional techniques dueto rapid work hardening. After the first machining pass, work hardening tends to plastically deform either the workpiece or the tool on subsequent passes. For this reason, age-hardened Inconel such as 718 are machined using an aggressive but slow cut with a hard tool, minimizing the number of passes required.

Property	21^{0}C	540 ^{0}C	650^{0}C	760^{0}C	870^{0}C
Yield strength (MPa)	1185	1065	1020	740	330
Ultimate tensile strength(MPa)	1435	1275	1228	950	340
Elastic modulus (GPa)	200	171	163	154	139
Specific heat capacity(J/Kg K)	430	560	----------	----------	645
Thermal conductivity(W/mK)	11.4	19.6	----------	----------	24.9
Coefficient of thermal expansion	----------	14.4	----------	----------	----------
Melting range (^{0}C)	1260-1335				
Density (Kg/m3)	8220				

Table 2.1 Physical properties of Inconel 718

Ni	Fe	Cr	Mo	Nb	Ti	Al	C	Mn	Si
52.5	18.5	19	3	5.1	0.9	0.5	0.04	2	0.2

Table 2.2. Chemical composition of Inconel 718 (%wt)

3.MATERIAL MODEL

The **johnson-cook model** as given in equation estimates the work Material flow stress as a product of strain, strain rate, and temperature effects, *i.e.*, work hardening and thermal softening The Johnson-Cook model has two principal elements: plasticity and damage initiation. The plasticity model prescribes the dependency of plastic flow stress $\bar{\sigma}$ on equivalent plastic strain $\bar{\varepsilon}$, equivalent plastic strain rate $\dot{\bar{\varepsilon}}$, and temperature: where *A*, *B*, *C*, and *m* are constants; *n* is strain hardening exponent; $\dot{\bar{\varepsilon}}/\dot{\bar{\varepsilon}}_0$ is the normalized equivalent plastic strain rate (typically normalized to a strain rate of 1.0 s^{-1}); and $\hat{\theta}^m$ is the homologous temperature defined as

$$\bar{\sigma} = \left(A + B\bar{\varepsilon}^n\right)\left[1 + C\ln\left(\frac{\dot{\bar{\varepsilon}}}{\dot{\bar{\varepsilon}}_0}\right)\right]\left(1 - \hat{\theta}^m\right)$$

A (Mpa)	B (Mpa)	C	n	m	- $\dot{\varepsilon}_0$ (1/s)	Room temperature (c)	Melting temperature (c)
450.0	1700.0	0.017	0.65	1.3	0.001	20.0	1297.0

Table. 3.1Johnson-Cook material constants for Inconel 718

4. FINITE ELEMENT SIMULATION USING DEFORM 2D

The commercial FEA software DEFORM 2D, a Lagrangian implicit code, was developed to simulate the orthogonal cutting process of Inconel 718 nickel alloy (DEFORM user manual, 2010). Finite element model of the orthogonal cutting process was developed and was composed of the workpiece and the tool. The workpiece was initially meshed with 8000 isoparametric quadrilateral elements, while the tool, modelled as rigid, was meshed and subdivided into 1000 elements. A plane-strain coupled thermo-mechanical analysis was performed using orthogonal assumptions.

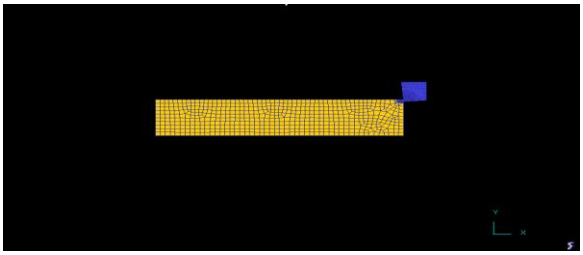

Table 4.1 shows the meshing of work piece and tool holder

5. RESULTS AND DISCUSSION

The finite element results for effective stress, strain, temperature distribution and damage with the input material model for different tool nose radius are presented in this chapter. The analysis is presented for cutting speed of 50 m/min and feed rate of 0.1 mm/rev for all different tool nose radius values (0.6, 0.8 & 1.0 mm).the cutting speed and feed rate at constant in this study. The FE output was observed at nearly steady state conditions in the study.

5.1 STRESS ANALYSIS

The von mises stress plot for effective stress distribution for 0.6, 0.8 & 1.0 mm tool nose radius are shown in figures 5.1 to 5.3. The negative rake angle causes the greater stress on the work material and the tool at the point of contact. The stress on the machined surface is residual in nature while stress value is decreased around the uncut surface and the deformed chip.

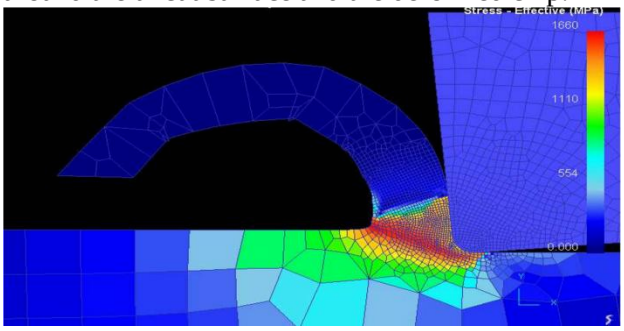

Fig 5.1 stress distribution at 0.6mm nose radius

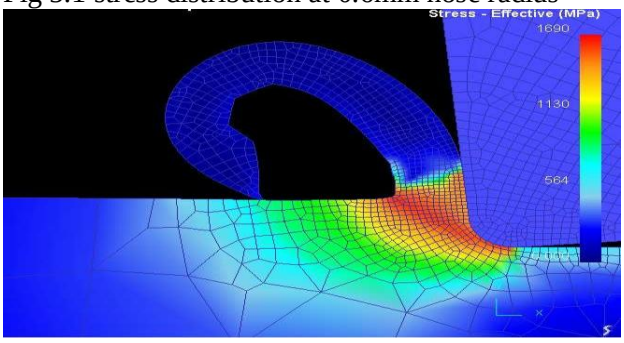

Fig 5.2 stress distribution at 0.8mm nose radius

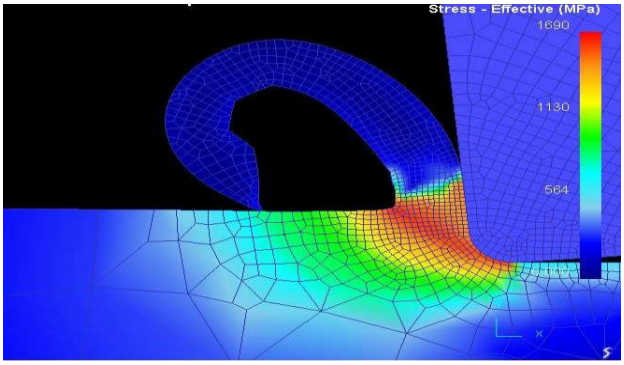

Fig 5.3 stress distribution at 1.0mm nose radius

5.2 STRAIN DISTRIBUTION

Figures 5.4 to 5.6 show the predicted effective strain distribution for 0.6, 0.8 & 1.0 mm tool nose radius values. The plastic strain is higher at the primary zone followed by the secondary shear zone and least at the free end of the chip. The chips shows regions of high and low strain across the chip thickness, suggesting a complex chip formation mode which results in serration and segments at low cutting speed machining. In other materials this phenomenon is presented only in high cutting speed machining. The higher stress near the shear plane for radius

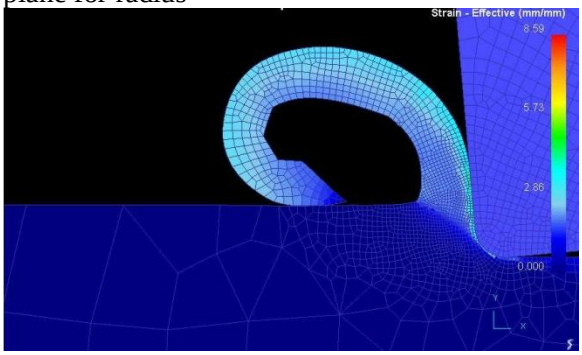

Fig 5.4 strain distribution at 0.6mm nose radius

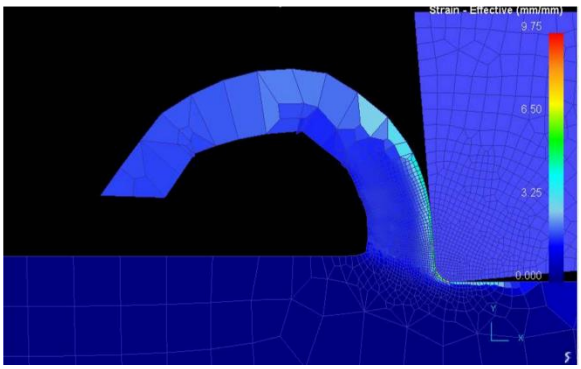

Fig 5.5 strain distribution at 0.8mm nose radius

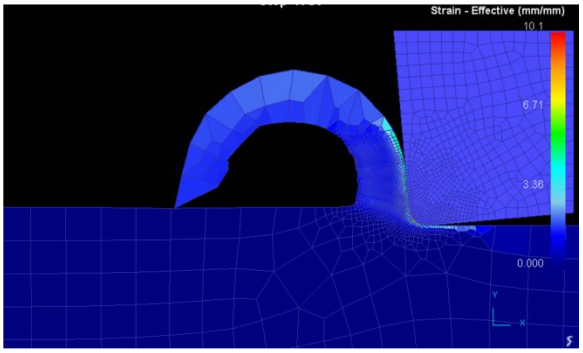

Fig 5.6 strain distribution at 1.0mm nose radius

1.0mm and 0.8mm should suggest higher deformations, but only 0.8mm replicates this proposition. 1.0mm and 0.8mm shows higher deformation at the shear plane tool chip contact respectively. It can be concluded that the nose radius 0.8mm with an optimized strain hardening exponent 'n' is a good tool for predicting plastic strain path of nickel alloy.

5.3 TEMPERATURE DISTRIBUTION

Figures 5.7 to 5.9 show that the temperature distribution for the various nose radius heatTransfers in the machining process takes place primarily in the shear zone was the plasticWork is converted into heat and the chip tool interface where the frictional heat is generated

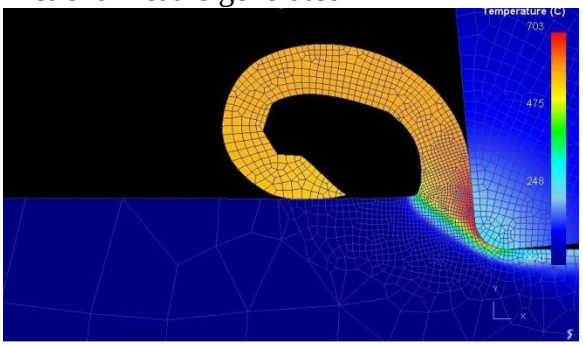

Fig 5.7Temperature distribution at 0.6mm nose radius

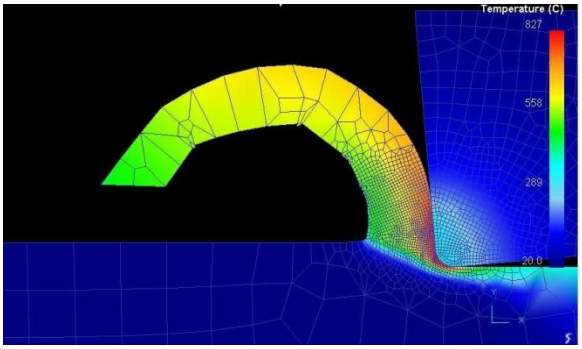

Fig 5.8 Temperature distribution at 0.8mm nose radius

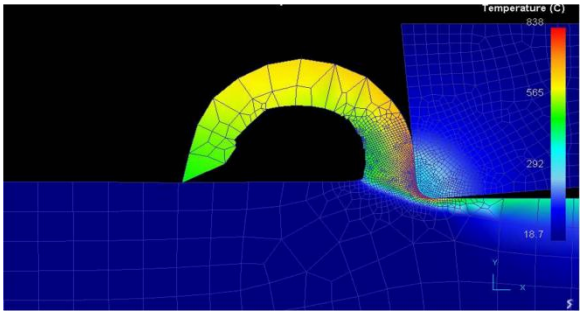

Fig 5.9 Temperature distribution at 1.0mm nose radius

5.4 DAMAGE DISTRIBUTION

Figure 5.10 and 5.11 show that damage value distribution in the chip during cutting of Inconel 718. The location of a larger damage value is correctly corresponding to the above Discussed stress state in chip segmentation. It can be seen that high damage value is located at a different region as the nose radius changes.

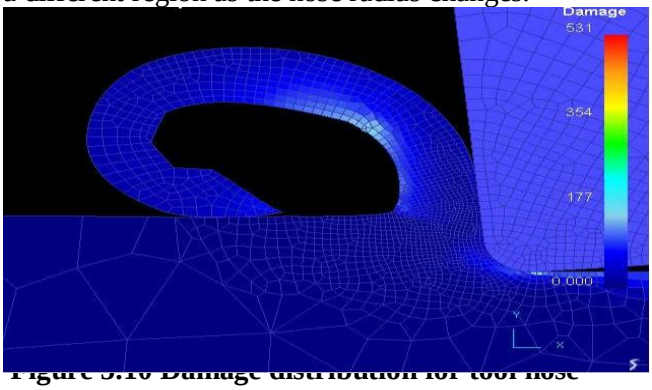

Figure 5.10 Damage distribution for tool nose radius of 0.6 mm

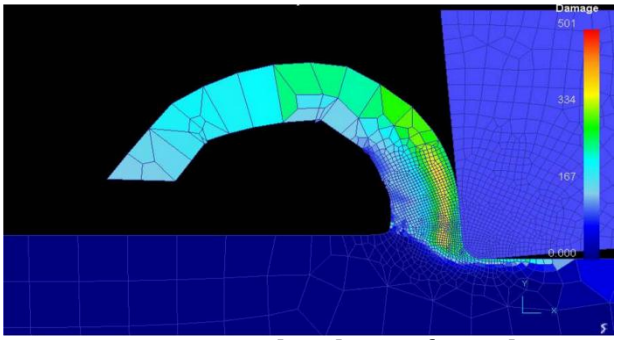

Figure 5.11 Damage distribution for tool nose radius of 0.8 mm

6. REFERENCES

1. Akhyar, *et.al.*, (2008), "Application of Taguchi method in the optimization of turning parameters for surface roughness." International journal of science, engineering and technology- vol 1 no3:2008

2. Childs, *et al.*, "Metal machining theory and application". Arnold, London, 2000.

3. Deshayes, Mabrouki, Lvester, and Rigal., (2004), "Serrated chip morphology and comparison with finite element simulations". ASME International mechanical Engineering congress and Exposition, Nov 13-20; 2004.

4. Duan, Dou, Cai, and .LI., (2009)," Finite element simulation and experiment of chip formation process during high speed machining of AISI 1045 hardened steel". International journal of recent trends in engineering vol1 no:5 may 2009.

5. Ezugwu, Bonney, Yamane., (1999) "The machinability of nickel based alloys: a review". Journal of material processing technology 86 (1999) 17-44

6. Fang and Wu, " A comparative study of cutting forces in high speed machining of Ti-6Al-4V and Inconel 718 with round cutting edge". Journal of material processing technology, 209(2009) 4385-4389.

7. Jiang Hua, Rajiv Shivpuri,(2004), "Prediction of chip morphology and segmentation during the machining of Titanium alloy". Journal of materials process technology 150(2004) 123-133.

8. Komanduri and Schroeder.,*(1986)*, "On shear instability in machining a NickelIron base super alloy", Transaction of ASME, Journal of Engineering for Industry 108 (1986) 93-100.

9. Marurich, and Askari., (2000), "modelling residual stress and work piece quality in machined surface.

10. Marurich, and Askari (2001), "simulation and analysis of chip breakage in turning process" 28 march 2001

11. Obikawa and andUsi (1998). "computational machining of Titanium alloy- finite element modelling and few results". Journal of manufacturing science and Engineering, may 1996, volume 118.

12. Ozel, and Ultan (2012) "Prediction of machining include residual stresses in turning of Titanium and Nickel based alloy with experiments and finite element simulations". CIRP Annals- manufacturing technology 61(2012)547-550.

13. Pawade, Harshad A Sonawane, Suhas . s. Joshi (2009)," an

analytical model to predict specific shear energy in high speed turning of Inconel 718". International journal of machine tools & manufactures. 42(2009)979-999.